

WATER TRAPPING ON TIDALLY LOCKED TERRESTRIAL PLANETS REQUIRES SPECIAL CONDITIONS

JUN YANG¹, YONGGANG LIU², YONGYUN HU³, AND DORIAN S. ABBOT¹

¹ Department of Geophysical Sciences, University of Chicago, Chicago, IL 60637, USA; junyang28@uchicago.edu

² Woodrow Wilson School of Public and International Affairs, Princeton University, Princeton, NJ 08544, USA

³ Laboratory for Climate and Atmosphere–Ocean Studies, Department of Atmospheric and Oceanic Sciences, School of Physics, Peking University, Beijing, China

Received 2014 September 6; accepted 2014 October 28; published 2014 November 12

ABSTRACT

Surface liquid water is essential for standard planetary habitability. Calculations of atmospheric circulation on tidally locked planets around M stars suggest that this peculiar orbital configuration lends itself to the trapping of large amounts of water in kilometers-thick ice on the night side, potentially removing all liquid water from the day side where photosynthesis is possible. We study this problem using a global climate model including coupled atmosphere, ocean, land, and sea ice components as well as a continental ice sheet model driven by the climate model output. For a waterworld, we find that surface winds transport sea ice toward the day side and the ocean carries heat toward the night side. As a result, nightside sea ice remains $\mathcal{O}(10\text{ m})$ thick and nightside water trapping is insignificant. If a planet has large continents on its night side, they can grow ice sheets $\mathcal{O}(1000\text{ m})$ thick if the geothermal heat flux is similar to Earth's or smaller. Planets with a water complement similar to Earth's would therefore experience a large decrease in sea level when plate tectonics drives their continents onto the night side, but would not experience complete dayside dessiccation. Only planets with a geothermal heat flux lower than Earth's, much of their surface covered by continents, and a surface water reservoir $\mathcal{O}(10\%)$ of Earth's would be susceptible to complete water trapping.

Key words: astrobiology – planets and satellites: detection – planets and satellites: general

Online-only material: color figures

1. INTRODUCTION

Liquid water is necessary for all known life forms (Kasting 2010). This has led to a definition of the habitable zone of a star as the region around it where a planet can maintain liquid water at its surface. The habitable zone is determined by radiative calculations (Kasting et al. 1993, 2014), assuming the functioning of the silicate-weathering feedback (Walker et al. 1981). A planet that is in the habitable zone, however, will not necessarily have surface water because of the vagaries of water delivery during planet formation (Morbidelli et al. 2000) and poorly understood processes that determine the distribution of water between the surface and the mantle (Cowan & Abbot 2014). While too little water is certainly a problem for life as we know it, too much water is likely problematic as well. If a planet has so much water that its continents are submerged, the silicate-weathering feedback cannot function (Abbot et al. 2012), undermining climate stability, and it may be difficult for life to get started because of a lack of suitable environments (Ward & Brownlee 2000). An understanding of the processes that determine the size of the surface liquid water reservoir is therefore essential for understanding planetary habitability.

Since M stars are the most common type of star in the galaxy, it is important to study issues relevant to the habitability of planets orbiting them. M-star habitable zone planets may be very dry because of inefficient scattering of water-bearing planetesimals from beyond the ice line into the habitable zone during planetary formation (Lissauer 2007; Raymond et al. 2007). Additionally, planets orbiting small M stars that start with large eccentricities could suffer massive heating due to tidal dissipation and lose their water via atmospheric escape (Barnes et al. 2013), and the strong stellar activity of M stars may strip the water and atmospheres of habitable zone planets (Lammer et al. 2007).

One issue of particular importance is that due to increased tidal interactions in closer orbits, planets in the habitable

zones of M stars will tend to have tidally locked orbital configurations, with one side always facing the star and the other side in permanent darkness (Kasting et al. 1993). A global atmospheric circulation with upwelling in the substellar region and downwelling in the rest of the planet will tend to transport water from the day side to the night side (Joshi et al. 1997; Merlis & Schneider 2010; Edson et al. 2011) and could lead to the trapping of a surface water reservoir on the cold night side as solid ice (Heath et al. 1999; Joshi 2003). Recent calculations using one-dimensional (1D) ice sheet dynamical and thermodynamical constraints have suggested that a sizable fraction of Earth's oceans (equivalent to $\approx 400\text{--}900\text{ m}$ of water distributed globally, or $\approx 15\%\text{--}35\%$ of Earth's globally distributed surface water complement of 2700 m) could be sequestered on the night side in this way (Menou 2013). These water traps in cold regions may be so effective that they could persist even if the planet receives more insolation than the traditional runaway greenhouse limit (Leconte et al. 2013).

As mentioned by Joshi (2003), Menou (2013), and Hu & Yang (2014), additional processes including ocean, sea ice, and three-dimensional (3D) ice sheet dynamical effects must be considered to fully address water trapping on the night side of tidally locked planets. For example, in the polar regions of Earth, the transport of sea ice into warmer regions and ocean heat transport (OHT) underneath sea ice prevent sea ice from growing thicker than $\approx 5\text{ m}$ (Lepparanta 2005). If such processes operate effectively on tidally locked exoplanets, as suggested by the simulations of Hu & Yang (2014), a shallow ocean could persist with a thin veneer of sea ice on the night side. The goal of this Letter is to address water trapping using both a 3D global climate model that interactively couples ocean, atmosphere, sea ice, and land, as well as a 3D thermo-mechanical ice sheet model. Our model results indicate that (1) water trapping is unlikely on planets without continents if they have at least a few percent of Earth's water complement and (2) water trapping would only

be possible on planets with continents if those continents cover much of the night side, the planet has about 10% of Earth’s water complement or less, and the geothermal heat flux (GHF) is lower than Earth’s.

2. METHODS

We perform climate simulations with the Community Climate System Model version 3.0 (CCSM3; Collins et al. 2006), which was originally developed by the National Center for Atmospheric Research to study the climate of Earth. The model contains four coupled components: atmosphere, ocean, sea ice, and land. The atmosphere component calculates atmospheric circulation and parameterizes sub-grid processes such as convection, precipitation, clouds, and boundary-layer mixing. The ocean component computes ocean circulation using the hydrostatic and Boussinesq approximations. The sea ice component predicts ice fraction, ice thickness, ice velocity, and energy exchanges between the ice and the atmosphere/ocean (Briegleb et al. 2004). The land component calculates surface temperature, soil water content, and evaporation.

We modify CCSM3 to simulate the climate of habitable planets around M stars following Rosenbloom et al. (2011), Liu et al. (2013), and Hu & Yang (2014). The stellar spectrum we use is a blackbody with an effective temperature of 3400 K. We employ planetary parameters typical of a super-Earth: a radius of $1.5 R_{\oplus}$, gravity of $1.38 g_{\oplus}$,⁴ and an orbital period of 37 Earth days. The orbital period of habitable zone planets around M stars is roughly ≈ 10 –100 days (Edson et al. 2011). We set the insolation⁵ to 866 W m^{-2} and both the obliquity and eccentricity to zero. The atmospheric surface pressure is 1.0 bar, including N_2 , H_2O , and 355 ppmv CO_2 .⁶ We set the albedo of sea ice to 0.3 and snow to 0.6, lower than those on Earth because of the redshifted stellar spectrum. We set the seawater freezing point to $-1.8 \text{ }^{\circ}\text{C}$. We use three different continental configurations: (1) a waterworld (with no continents) with a constant ocean depth of 325, 815, or 3800 m; (2) an idealized supercontinent with a uniform elevation of 100 m above sea level, covering the entire night side and an ocean with a constant depth of 3800 m on the day side; and (3) modern Earth’s continental topography and ocean bathymetry and a substellar point in either the Atlantic Ocean, Pacific Ocean, or Africa.

The atmospheric component of CCSM3 has a horizontal resolution of $3^{\circ}75 \times 3^{\circ}75$ with 26 vertical levels ranging from the surface to $\approx 30 \text{ km}$. The ocean and sea ice components have a $3^{\circ}6$ resolution in the west–east direction and a variable resolution in the south–north direction, ranging from $0^{\circ}9$ near the equator to 4° at high latitudes. The ocean has 25 vertical layers. We run the model until it reaches statistical steady state (≈ 500 –2000 Earth years), after which we average all results for 100 yr.

To calculate the thickness of ice sheets over continents, we use the CCSM3 surface temperature and precipitation⁷ output to drive a separate ice sheet model. The ice sheet model we use is the University of Toronto Glacier Systems model

(Tarasov & Peltier 1999, 2005; Liu & Peltier 2013), which is a 3D thermo-mechanical model that makes the shallow-ice approximation. The ice sheet model calculates ice flow using a standard Glen’s flow law with a temperature-dependent flow factor and includes basal sliding when the basal temperature is near the pressure melting point. If basal melting occurs, the melt water is assumed to be carried by subglacial streams to the ocean immediately.⁸ No surface melting occurs on the night side because the surface temperature is always less than the melting point.

We use the same planetary parameters in the ice sheet model as in CCSM3. The spatial resolution of the model is $0^{\circ}5 \times 0^{\circ}5$, which corresponds to $80 \times 80 \text{ km}$. The mean density of the bedrock, which is used to calculate its isostatic deformation, is 3300 kg m^{-3} (Earth’s value). We test the influence of the GHF by varying it from 0.01 to 1.0 W m^{-2} . The average GHF on continents of modern Earth is 0.07 W m^{-2} (Davies & Davies 2010). We assume an atmospheric lapse rate of 7.5 K km^{-1} , and sensitivity tests show that the equilibrium ice thickness is insensitive to the lapse rate because no surface melting occurs. Sensitivity tests also show that our results are insensitive to flow and basal sliding enhancement factors.

3. THIN SEA ICE OVER OCEAN

We begin by discussing the sea ice thickness on a waterworld with a uniform ocean depth of 325 m, which is below the threshold for which all of the water would be trapped on the night side if ocean and sea ice dynamics are neglected (Menou 2013). In our calculations including ocean and sea ice dynamics, we find a maximum sea ice thickness of only 5.4 m (Figure 1(a)), so very little of the planetary water complement is sequestered as ice on the night side.⁹

To understand the thinness of the nightside sea ice, we need to investigate the dominant balance in the sea ice time-evolution equation. The sea ice thickness is determined by a balance between thermodynamic growth on the night side and the dynamical export of this ice to the day side where it is melted (Figure 2(a)). Ice growth on the night side is primarily due to freezing at the ice bottom (Figure 2(b)). Dayside ice melting occurs both at the ice top due to warm air (Figure 1(c)) and at the ice bottom as a result of warm seawater (Figure 1(e)). The simulated ocean circulation of tidally locked waterworlds is characterized by strong eastward currents along the equator around the planet (Figure 1(g); see also Hu & Yang 2014). This ocean circulation transports heat from the warm substellar region to the night side, effectively thinning the ice there, and it becomes stronger the deeper the ocean (for example, see the 815 m depth case in Figure 1(h), and the 3800 m depth case in Figures 2 and S3 of Hu & Yang 2014). The flow of sea ice from the night side to the day side is primarily driven by surface winds (Figure 2(c)), which blow toward the relatively warm substellar region. Sea ice dynamics are important enough that the nightside sea ice grows to 200–400 m thick when they are artificially switched off (not shown). Since sea ice dynamics can differ among climate models (Bitz 2008) and different schemes are required for ice hundreds of meters thick (Tziperman et al. 2012), it is important to check these results in other models.

⁴ We also did three experiments with Earth’s radius and gravity and different stellar fluxes (866, 966, and 1066 W m^{-2}). We found that as long as the planet does not enter a globally ice-covered snowball state, the sea ice thickness does not exceed $\mathcal{O}(10 \text{ m})$.

⁵ This compares to $\approx 1370 \text{ W m}^{-2}$ for Earth and $\approx 590 \text{ W m}^{-2}$ for Mars.

⁶ We tested lower CO_2 and stellar flux values for which the model is closer to complete glaciation, and found that sea ice is thin in these cases as well.

⁷ We neglect sublimation because it is at least an order of magnitude less than precipitation on the night side.

⁸ This model does not calculate the specific paths melt water would take as it flows to the ocean; however, this is unlikely to affect the equilibrium global ice volume.

⁹ The model we use cannot calculate ocean dynamics for “oceans” as shallow as $\mathcal{O}(10 \text{ m})$, but it is possible that oceans this shallow could be trapped on the night side as ice.

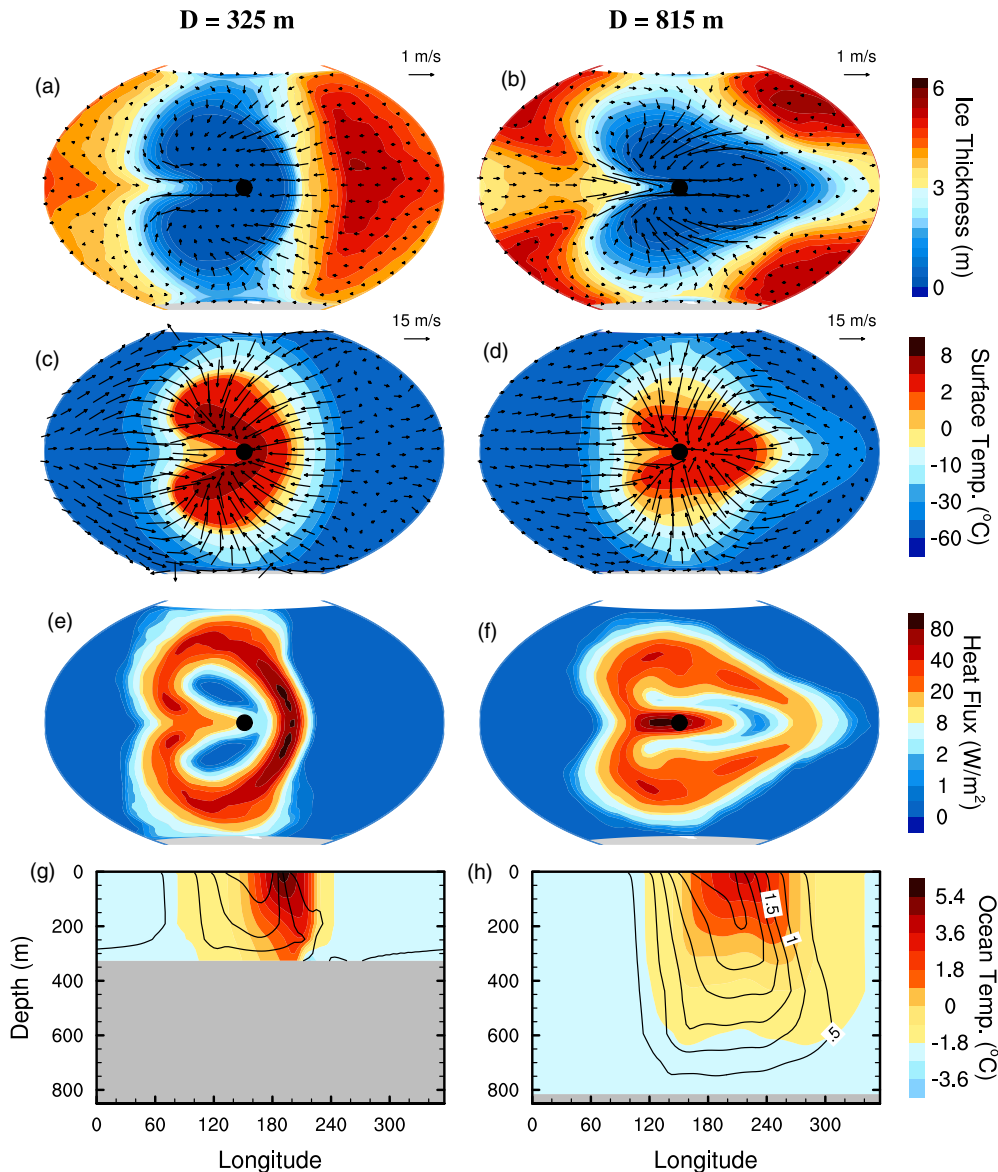


Figure 1. Climates of tidally locked waterworlds with ocean depths (D) of 325 m (left panels) and 815 m (right panels), simulated by CCSM3. (a) and (b) Sea ice thickness (color shaded) and velocity (vector); (c) and (d) surface air temperature (color shaded) and surface winds (vector); (e) and (f) heat flux from ocean to sea ice due to ice bottom melting; and (g) and (h) ocean temperature (color shaded) and west–east velocity (contours with an interval of 0.5 m s^{-1}), averaged between 5°S and 5°N . The black dot in panels (a)–(f) is the substellar point. Note that the color scales for panels (e)–(h) are not linear.

(A color version of this figure is available in the online journal.)

To investigate the ability of continents to disrupt ocean and sea ice flow, and consequently increase sea ice thickness, we repeat the 3800 m ocean depth simulation but add continental barrier(s) that are south–north oriented, narrow, and extend to the bottom of the ocean. When we add one barrier spanning the western terminator, the nightside sea ice thickness increases only slightly (not shown). When we add an additional barrier on the eastern terminator, so that both OHT and sea ice flow between the night and day sides are completely blocked, the sea ice thickness reaches $\mathcal{O}(1000 \text{ m})$. This confirms that ocean and sea ice dynamics are essential for maintaining thin sea ice and preventing water trapping on a waterworld. These simulations also demonstrate that water trapping of a significant ocean would be possible if a planet had continents positioned so that they completely disrupted OHT and sea ice flow between its day and night sides.

On modern Earth, continents provide large south–north barriers, but do not completely obstruct ocean and sea ice flow. Since this may represent a more realistic possible continental configuration than complete barriers, we repeat the simulations using modern Earth’s continental configuration. In general, sea ice stays $\mathcal{O}(10 \text{ m})$ thick, although it can grow to $\mathcal{O}(100 \text{ m})$ thick in small regions that are strongly isolated by continents, such as the Caribbean Sea, Baffin Bay, and the Mediterranean Sea (Figure 3(a)). Even small gaps in continental coverage, such as the Drake Passage between South America and Antarctica and the Bering Strait between Asia and North America, allow efficient transport of sea ice into warm regions where it can melt.

4. ICE SHEET THICKNESS OVER A CONTINENT

We begin our investigation of ice sheets on nightside continents with the idealized case of a supercontinent that spans the

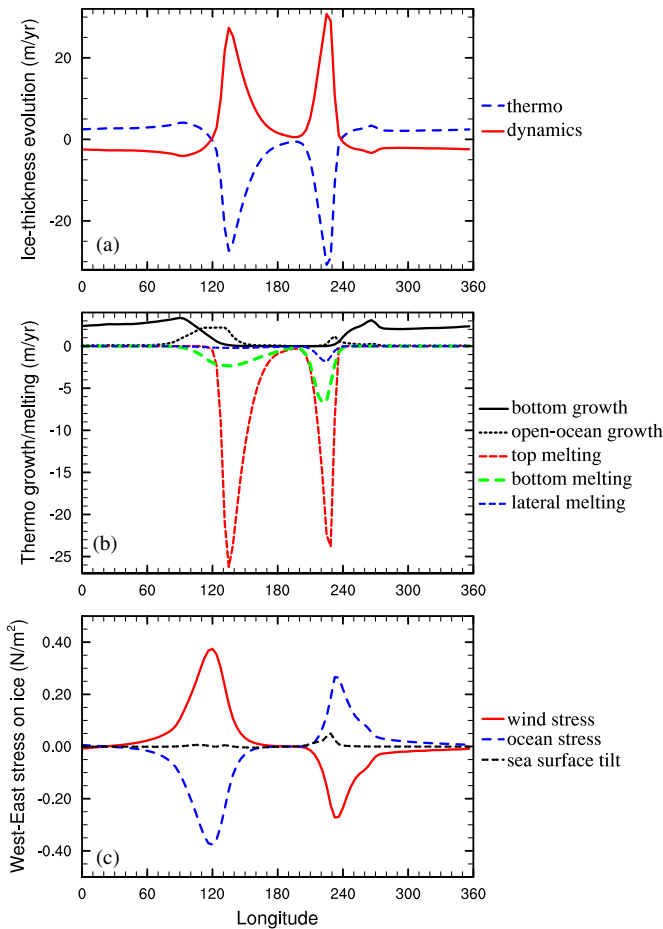


Figure 2. Processes determining sea ice thickness on a tidally locked waterworld with an ocean depth of 325 m. (a) Ice thickness evolution due to thermodynamics (blue) and dynamics (red). (b) Subcomponents of the thermodynamics: bottom ice growth, open-ocean ice growth, top ice melting, bottom ice melting, and lateral ice melting. The ice-top snow-to-ice conversion term is $\approx 2\text{--}3$ orders of magnitude smaller than other terms, so it is not shown. (c) West-east stress on the ice: wind stress, ocean stress, and a force due to sea surface tilt. The Coriolis force and internal ice stress are very small, so they are not shown. All variables are averaged between 5°S and 5°N .

(A color version of this figure is available in the online journal.)

entire night side, which is optimal for water trapping. Our simulations confirm that the ice volume trapped on the continent is critically dependent on the magnitude of the GHF, as suggested in Menou (2013) and Leconte et al. (2013). The average ice thickness¹⁰ on the night side is 3445 m if the GHF is 0.05 W m^{-2} , and decreases to 387 m if the GHF is 0.5 W m^{-2} (Figure 4). For a GHF similar to Earth’s, a dayside ocean of $\approx 2880 \text{ m}$ (or $\approx 1440 \text{ m}$ distributed globally, about half of Earth’s water complement) could be trapped on the nightside supercontinent. This estimate agrees fairly well with that obtained by Menou (2013) using simpler ice sheet models that have the benefit of elucidating the scaling of ice sheet thickness with a variety of physical parameters that will vary among exoplanets. If the GHF is significantly higher (as one might expect on a super-Earth), only a small ocean a few hundred meters deep could be trapped, even on a continent encompassing the entire night side.

The mean ice sheet thickness is well approximated by the 1D energy balance limit (e.g., Abbot & Switzer 2011) if the ice sheet is thinner than $\approx 2000 \text{ m}$ (Figure 4(e)). This is because ice flow is slow and is concentrated around the ice sheet edges (Figure 4(c)), so it does not have a significant effect on the equilibrium ice thickness. When the ice sheet is thicker than $\approx 2000 \text{ m}$, the ice flow speed increases and large regions of the interior of the ice sheet are affected by ice flow. This can be inferred from the surface slope of the ice sheet (Figure 4(d)) based on the fact that the ice speed is roughly proportional to the cube of the surface slope. As a result, the increased export of land ice toward the ocean prevents the ice sheet from growing to the thickness estimated based on the 1D limit (Figure 4(e)).

When we use modern Earth’s continental configuration, a GHF of 0.05 W m^{-2} , and the substellar point located in the central Pacific Ocean, the globally distributed ice sheet thickness is $\approx 470 \text{ m}$ (Figure 3(b)). This is 32% of the water trapped by the idealized supercontinent spanning the entire night side (for reference, 36% of the night side is covered by continents in this simulation), or 18% of modern Earth’s water complement. Moving the substellar point from the Pacific Ocean to the Atlantic Ocean or Africa yields lower global-mean ice

¹⁰ The ice sheets on Greenland and Antarctica on modern Earth are generally a few kilometers thick. The sea level would rise by $\approx 70 \text{ m}$ if they were to melt completely (Marshall 2012).

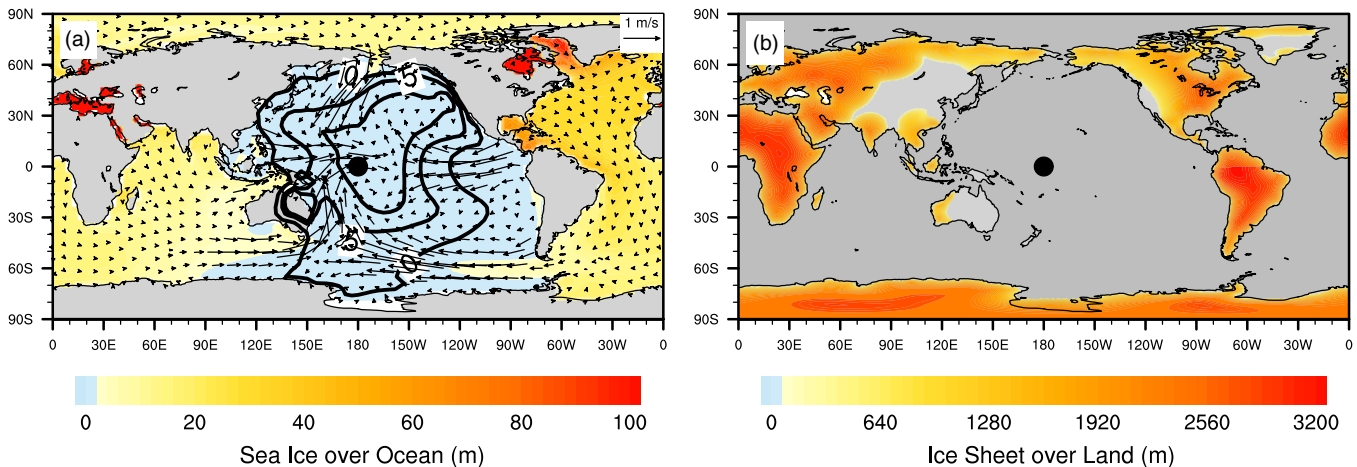


Figure 3. Thicknesses of sea ice over ocean (a) and ice sheet over land (b) for a tidally locked planet with modern Earth’s continental configuration. In panel (a), vectors show the sea ice velocity, and thick black contours indicate surface air temperatures of 0°C , 5°C , and 7°C . In panel (b), the geothermal heat flux over continents is set to 0.05 W m^{-2} . If it were higher, the ice sheet would be much thinner and flatter. The black dot is the substellar point.

(A color version of this figure is available in the online journal.)

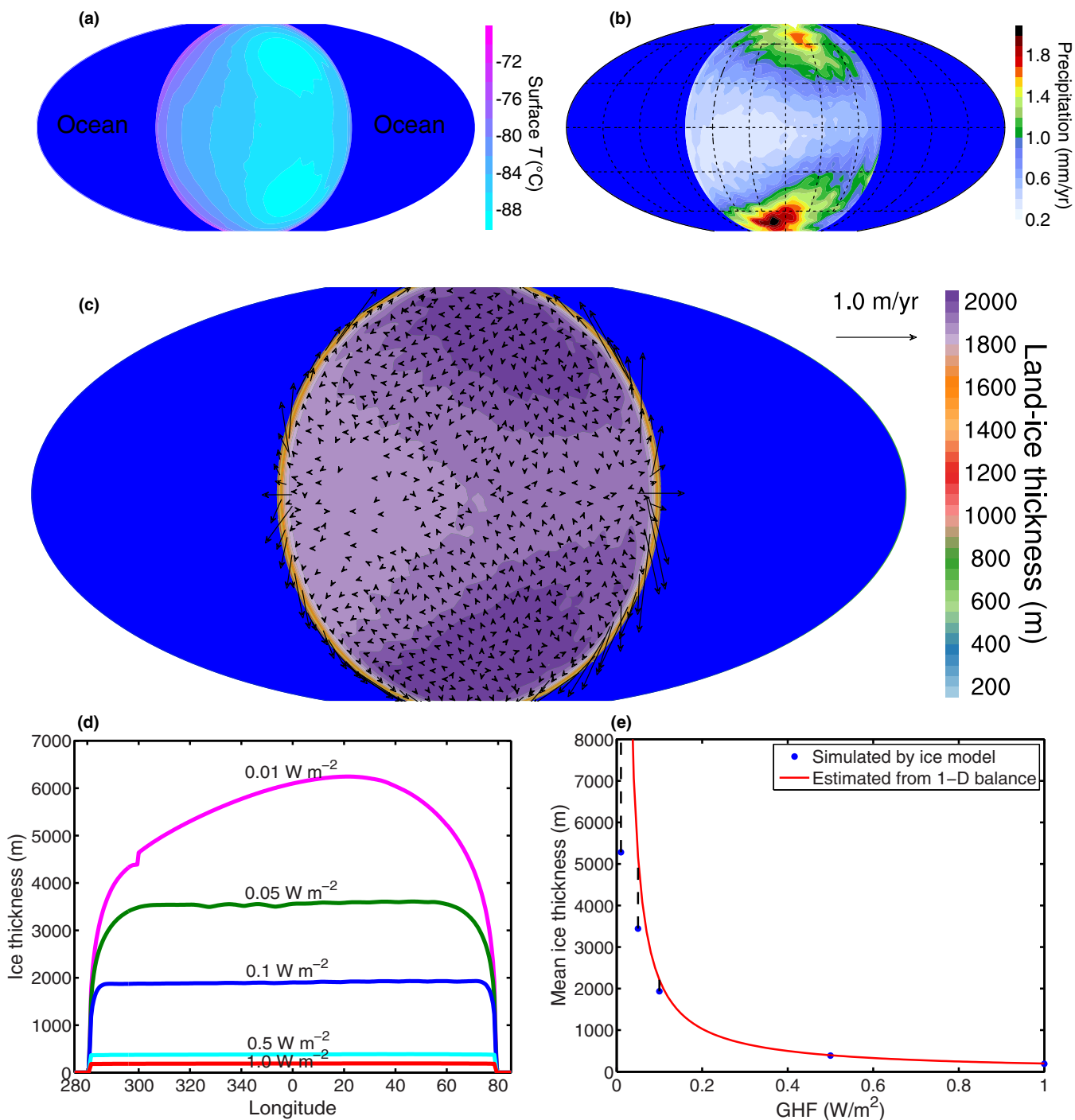


Figure 4. Climate and ice sheet over a supercontinent spanning the entire night side. (a) Surface temperature and (b) precipitation over the continent, which are both used to drive the ice sheet model. (c) Ice sheet thickness (color shaded) and ice sheet flow velocity (vector) with a geothermal heat flux (GHF) of 0.1 W m^{-2} . (d) Ice sheet thickness along the equator with GHF ranging from 0.01 to 1.0 W m^{-2} . (e) Nightside mean ice sheet thickness calculated by 1D energy balance limit (red line) and by the 3D ice sheet model (dots). The vertical dashed lines in panel (e) indicate the overestimate of ice sheet thickness by the 1D balance limit.

(A color version of this figure is available in the online journal.)

sheet thicknesses and similar global-mean sea ice thicknesses (not shown).

5. CONCLUSION

We have applied sophisticated global climate and ice sheet models to the question of water trapping on the night side of tidally locked terrestrial planets. We found that OHT and sea ice dynamics are likely to limit nightside sea ice thickness and

prevent water trapping on a planet with no continents (shown schematically in Figure 5(a)). If a planet has continents that completely block ocean flow and sea ice transport between the day and night sides, the sea ice thickness can reach the kilometer scale, but even small gaps in this blocking keep the sea ice thin. Additionally, we found that ice sheets on nightside continents can approach the kilometer scale (Figure 5(b)), although this would only limit the habitability of planets with surface water complements $\mathcal{O}(10\%)$ of Earth’s, very large

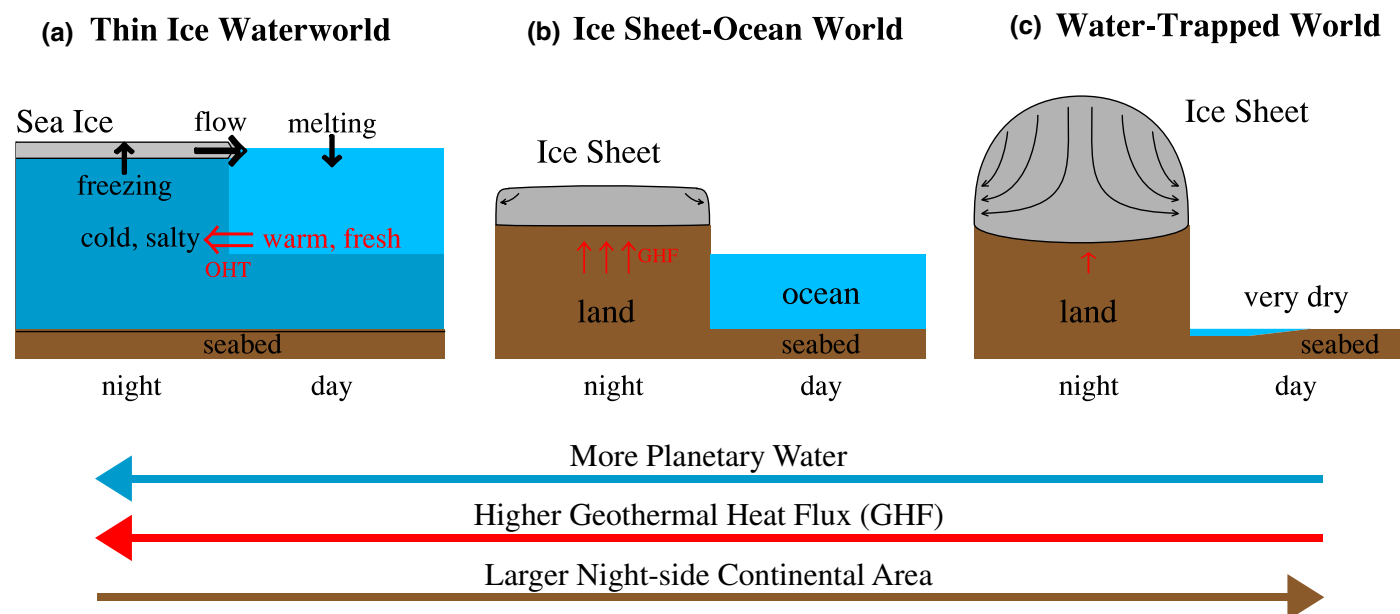


Figure 5. Schematic diagrams of (a) a planet with thin sea ice on the night side of a waterworld, (b) a planet with a small ice sheet on a nightside continent, and (c) a water-trapped world with a large nightside ice sheet. In panel (a), sea ice dynamics and ocean heat transport (OHT) keep the sea ice thin. In panel (b), the geothermal heat flux (GHF) is large enough to keep the ice sheet small so that it cannot trap all of the planet's water. In panel (c), GHF is small enough that almost all of the water is trapped on the nightside ice sheet, although subglacial streams and the melting of ice that flows across the terminator allow a small amount of water on the day side. This last configuration will only be possible if the GHF is small, the planetary water complement is small, and there are relatively large continents located preferentially on the night side.

(A color version of this figure is available in the online journal.)

continents covering most of their night side, and a GHF smaller than Earth's (Figure 5(c)). Such planets would experience irregular moistening and desiccation of their day side as plate tectonics exchanges their continents between their day and night sides. It will be difficult to remotely detect the quantity of water trapped on the night sides of exoplanets, but it may be possible to determine whether the day sides are dry from the bond albedo or by studying the visible/near-infrared phase curves (e.g., Cowan et al. 2009), although clouds would complicate such observations (e.g., Yang et al. 2013).

We thank Dawei Li, Raymond T. Pierrehumbert, Jiping Liu, and Sergey Malyshev for helpful discussions. We thank Daniel Koll and Douglas MacAyeal for comments on an early version of this letter. Y.H. is supported by the National Natural Science Foundation of China (41025018 and 41375072). D.S.A. acknowledges support from an Alfred P. Sloan Research Fellowship.

REFERENCES

- Abbot, D. S., Cowan, N. B., & Ciesla, F. J. 2012, *ApJ*, **756**, 178
 Abbot, D. S., & Switzer, E. R. 2011, *ApJL*, **735**, L27
 Barnes, R., Mullins, K., Goldblatt, C., et al. 2013, *Asbio*, **12**, 225
 Bitz, C. M. 2008, Numerical Modeling of Sea Ice in the Climate System, http://www.atmos.washington.edu/~bitz/Bitz_draftchapter.pdf
 Briegleb, B. P., Bitz, C. M., Hunke, E. C., et al. 2004, Technical Note, Document NCAR/TN-463+STR (Boulder, CO: NCAR)
 Collins, W. D., Bitz, C. M., Blackmon, M. L., et al. 2006, *JCLI*, **19**, 2122
 Cowan, N. B., & Abbot, D. S. 2014, *ApJ*, **781**, 1
 Cowan, N. B., Agol, E., Meadows, V. S., et al. 2009, *ApJ*, **700**, 915
 Davies, J. H., & Davies, D. R. 2010, *SoIE*, **1**, 5
 Edson, A., Lee, S., Bannon, P., Kasting, J. F., & Pollard, D. 2011, *Icar*, **212**, 1
 Heath, M. J., Doyle, L. R., Joshi, M. M., & Haberle, R. M. 1999, *OLEB*, **29**, 405
 Hu, Y., & Yang, J. 2014, *PNAS*, **111**, 629
 Joshi, M. M. 2003, *Asbio*, **3**, 415
 Joshi, M. M., Haberle, R. M., & Reynolds, R. T. 1997, *Icar*, **129**, 450
 Kasting, J. F. 2010, *How to Find a Habitable Planet* (Princeton, NJ: Princeton Univ. Press)
 Kasting, J. F., Kopparapu, R., Ramirez, R. M., & Harman, C. E. 2014, *PNAS*, in press
 Kasting, J. F., Whitmire, D. P., & Reynolds, R. T. 1993, *Icar*, **101**, 108
 Lammer, H., Lichtenegger, H. I., Kulikov, Y. N., et al. 2007, *Asbio*, **7**, 185
 Leconte, J., Forget, F., Charnay, B., et al. 2013, *A&A*, **554**, A69
 Lepparanta, M. 2005, *The Drift of Sea Ice* (Heidelberg, Germany: Springer)
 Lissauer, J. J. 2007, *ApJL*, **660**, L149
 Liu, Y., & Peltier, W. R. 2013, *JGR*, **118**, 4410
 Liu, Y., Peltier, W. R., Yang, J., & Vettoretti, G. 2013, *CliPa*, **9**, 2579
 Marshall, S. J. 2012, *The Cryosphere* (Princeton, NJ: Princeton Univ. Press)
 Menou, K. 2013, *ApJ*, **774**, 51
 Merlis, T. M., & Schneider, T. 2010, *JAMES*, **2**, 13
 Morbidelli, A., Chambers, J., Lunine, J. I., et al. 2000, *M&PS*, **35**, 1309
 Raymond, S. N., Scalo, J., & Meadows, V. S. 2007, *ApJ*, **609**, 606
 Rosenbloom, N., Shields, C., Brady, E., Levis, S., & Yeager, S. 2011, Technical Note, Document NCAR/TN-483+STR (Boulder, CO: NCAR)
 Tarasov, L., & Peltier, W. R. 1999, *JGR*, **104**, 9517
 Tarasov, L., & Peltier, W. R. 2005, *Natur*, **435**, 662
 Tziperman, E., Abbot, D. S., Ashkenazy, Y., et al. 2012, *JGRC*, **117**, C05016
 Walker, J. C. G., Hays, P. B., & Kasting, J. F. 1981, *JGR*, **86**, 9776
 Ward, P. D., & Brownlee, D. 2000, *Rare Earth: Why Complex Life is Uncommon in the Universe* (New York: Copernicus Books)
 Yang, J., Cowan, N. B., & Abbot, D. S. 2013, *ApJL*, **771**, L45